University of Stavanger

Faculty of Science and Technology

MASTER'S THESIS

Study program/ Specialization: Master of Science in Petroleum Technology with specialization in Drilling and Well Technology	Spring semester, 2010 Open
Author: Olav Harstad Storebø	…… (Author's signature)
Faculty supervisor: Jan Aasen External supervisor: Jan Aasen	
Title of thesis: Experimental study on Woods' theory within buckling	
Credits (ECTS): 30 sp	
Key words: -Buckling -Woods' theory	Pages: 38 + enclosure: 38 Stavanger, 15.06.2010 Date/year

Preface

I would like to thank my supervisor Jan Aasen. He was the one who came with the idea to do an experimental study on what Woods had presented before. He has always been helpful throughout the thesis.

It was really exiting to do an experimental study in the thesis. There were not a former setup for this kind of test, and part of the thesis was used to design a setup to be able to complete the experimental tests. In the early part while I was trying to gather ideas and equipment to build the setup, I got a lot of help from the engineers at the university. I will also thank them, especially Sivert Drangeid who always gave me assistance when needed.

This thesis has given me a huge knowledge in the theory within buckling. I have also got the opportunity to come with ideas on how to design the setup used for the experimental study.

Table of contents

Nomenclature

A	Area
A_i	Area inside of tubing
A_o	Area outside of the tubing
A_{ni}	Area inside of nipple
A_{no}	Area outside of nipple
A_p	Area packer
E	Young's Modulus
F	Force
F_{fric}	O-ring friction force
F_f	Fictitious force
F_a	Actual force
F_R	Real force
F_E	Effective force
F_p	Packer force
F_{ap}	Axial force corresponding to the packer force
I	Second moment of Inertia
L	Length
ΔL	Length change
ΔL_1	Length change due to piston effect
ΔL_2	Length change due to helical buckling
ΔL_3	Length change due to ballooning effect
ΔL_6	Total length change
ΔL_p	Correspondent length change to the total length change to keep the tube end fixed
ΔL_f	Fictitious length change
ΔL_{pf}	Overall length change
MF	Measured force
p	Pitch
P	Pressure

P_i	Pressure inside tubing, internal pressure
P_o	Pressure outside tubing
P_e	Pressure outside tubing, external pressure
r	Radial clearance between hose and plexi tube
R	Ratio OD/ID of the tubing
w	Weight per unit
LBL_1	Lateral buckling limit
HBL_1	Helical buckling limit, Chen
HBL_2	Helical buckling limit, Miska/Cunha
v	Poisson ratio
σ	Stress
ε	Strain

Abstract

In this thesis an experimental study is conducted in an attempt to reproduce Woods' experimental findings. Woods' setup has a tube with internal and external pressures. The tube will buckle if the axial stress working on the tube is less than the other two principal stresses working in hoop and radial directions

The setup for the experimental work in this thesis is built from the bottom, and is improved over time. The current setup gives result comparable to Woods' experiment. The tube chosen in this thesis is a rubber hose. At the end of the tube a load cell to measure the force is present. The pressure inside the tube is increased with a pump, and the pressure is measured with a pressure gauge. After the completion of the setup several tests were conducted. The results from these tests were compared with available literature. The results from the experimental work and the theory is compared in the discussion part of the thesis

In the present work the outside pressure is zero. The rubber hose is filled with water and self-weight buckling resistance. Helical buckling occurred at 3 bar inside pressure; fully supported by Woods' theory.

From the experiment the tests shows that the buckling limits correlate well with the theory. The changes in length however are not very suitable with the theory. The theory presents equations for buckling of steel tubes, and in this thesis a rubber tube is used.

This thesis may be a foundation for similar and further experimental work done with metal tubes.

1 Theory

1.1 Buckling

Buckling is a failure mode of a structural member characterized by sudden failure due to compressive stresses. When axial compression forces are applied on a pipe and they are larger than the critical value for buckling, the pipe will buckle. First lateral buckling occurs, and if the compressive forces increases the pipe will go into a helix, and helical buckling has occurred[1]. The difference between lateral and helical buckling is shown in figure 1.

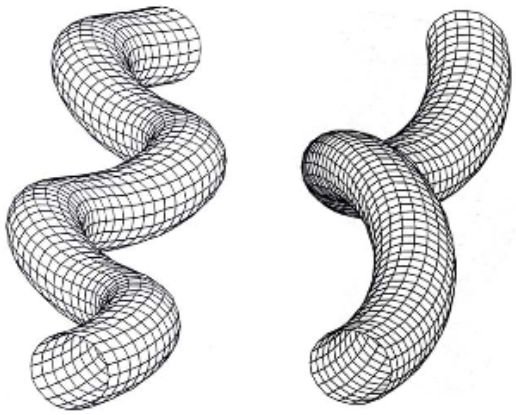

Figure 1: A pipe in lateral buckling deformation (figure to the left) and a pipe in helical buckling deformation (figure to the right.)

The critical value for lateral buckling, or the lateral buckling limit, *LBL*, in a horizontal well is derived by Dawson and Paslay[2] and is given by equation 1:

$$LBL = 2\sqrt{\frac{EIw}{r}} \qquad \text{(eq. 1)}$$

There are two different equations derived for the critical value for helical buckling, or the helical buckling limit, *HBL*, in a horizontal well. One is derived by Chen[3] and is in this

thesis called HBL_1. This is given in equation 2. The other helical buckling limit is derived by Miska and Cunha[4] and called HBL_2 and is given in equation 3:

$$HBL_1 = 2\sqrt{\frac{2EIw}{r}} \qquad \text{(eq. 2)}$$

$$HBL_2 = 4\sqrt{\frac{2EIw}{r}} \qquad \text{(eq. 3)}$$

1.2 Woods' experiment

In the paper "*The neutral zones in drill pipe and casing and their significance in relation to buckling and collapse*" written by A. Klinkenberg in 1951[5], H. B. Woods' experiment is described in the appendix. In a written discussion to the Klinkenberg paper, Woods presents his view on buckling stability and verifies the theory with results from buckling experiment. His setup is shown in figure 2. Woods' apparatus has different internal and external pressure, and the end of the tube terminates in a separate pressure chamber. It is assumed that there is a sliding leak proof fit outside the tube making the top pressure chamber separate. So there are three spaces with separate spaces.

The inside of the tube with the pressure P_i

The outside of the tube with the pressure P_e

The space above the tube at pressure P

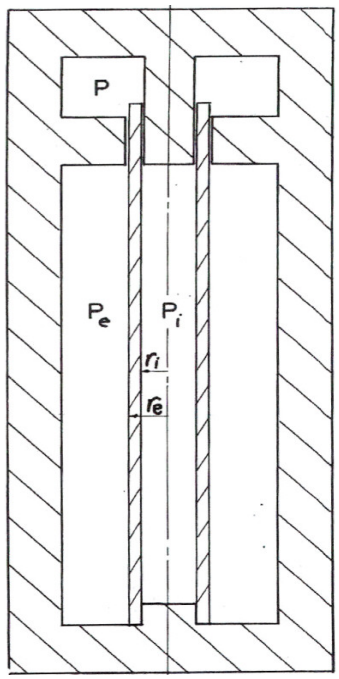

Figure 2: Woods experimental setup

Assumptions that are made in this experiment is that the tube is weightless, and that the length of the tube is great compared to its stiffness. If there is a small lateral movement of the tube at its middle, the top tube will slide down a small amount. If so there will be a change in the volume of each chamber. The external pressure chamber will decrease in volume while the internal and the top pressure chamber will increase in volume. It is assumed that the volume of each chamber is so large that a slight change in volume does not cause a change in pressure. Since there is a movement of the tube a work has been done.

A small displacement of the tube from equilibrium is defined, the equilibrium as stable if the change in potential energy is increasing, the equilibrium is neutral if there is not any change in potential energy, and that the equilibrium is unstable if there is a decrease in potential energy.

From these statements the equilibrium is stable if the axial stress is greater than the average of the other two principal stresses. The equilibrium is neutral if the axial stress is equal to the average of the other two principal stresses. The equilibrium is unstable and buckling may occur if the axial stress is less than the average of the other two principal stresses. This is truly pioneering work

Woods' experiment was conducted from this theory with a rubber tube and external and internal pressures, and the third pressure chamber open to the atmosphere. The experiment showed that if the external pressure was much over half of the internal pressure the tube remained straight. If the external pressure was about half of the internal pressure or less the tube would buckle. We see that outside pressure prevents buckling, while inside pressure causes buckling.

1.3 Real force and effective force

In this thesis the forces in compression are defined as positive, and the forces in tension are defined as negative. This sign convention is opposite to Woods and the same as Lubinski discussed below.

From the collected works of Arthur Lubinski[6] the helical buckling of tubing sealed in packers are explained. The Lubinski packer approach is thought to be applicable to the experimental setup in this thesis, although some modifications are needed. Helical buckling is when a pipe goes into a spiral. The pitch, p, is defined as the distance between the spirals just above the packer, where the compression of the tubing is largest. In this thesis there is a horizontal setup, and the compression is the same over the whole tube, so the pitch is here equal over the whole tube.

The pitch is given by equation 4:

$$p = \pi\sqrt{\frac{8EI}{F_E}} \qquad \text{(eq. 4)}$$

In the setup in the present work there is a piston effect at the nipple. Area $A_{no} - A_{ni}$ tries to extend the tube, while area $A_{no} - A_i$ has the opposite effect. The net area is A_i - A_{ni}. In figure 3 the nipple in the end of the hose and the area parameters are shown.

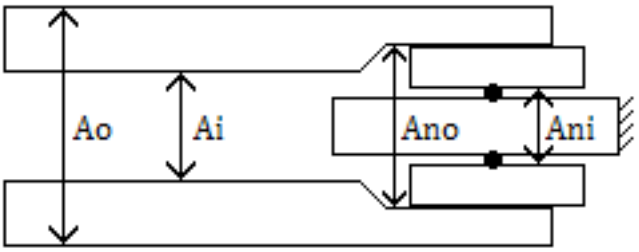

Figure 3: Nipple area of the setup in present work.

F_E is the effective force and is the same as the fictitious force, F_f, from Lubinski. Since there is no pressure outside the hose, the outside pressure is neglected and the packer area, A_p, is in this thesis given by the inside area of the nipple, A_{ni}. The effective force is given by equation 5:

$$F_E = F_f = A_{ni} \cdot P_i \qquad \text{(eq. 5)}$$

Lubinski also explains an actual force, F_a. This is the same as the real force, F_R, used in this thesis. This piston effect is given by equation 6:

$$F_R = F_a = -\left(A_i - A_{ni}\right)P_i \qquad \text{(eq. 6)}$$

The effective force, F_E, may also be calculated using equation 7. It is readily verified that this equation is the same as the equation for fictitious force from Lubinski, equation 5.

$$F_E = F_R + A_i P_i \qquad \text{(eq. 7)}$$

When the effective force becomes larger than the buckling limit, buckling occurs.

1.4 Length changes

Lubinski also describe the change in length of the tubing. The total length change, ΔL_6, is given by the length change caused by piston effect, the length change due to helical buckling, the length change due to ballooning effect and the length change due to temperature change. In this thesis there will be no changes in temperature so only the length change due to piston effect, helical buckling and ballooning effect is discussed. The total length change is given by equation 8, for a case with buckling. If there is no buckling, length change ΔL_2 is zero.

$$\Delta L_6 = \Delta L_1 + \Delta L_2 + \Delta L_3 \qquad \text{(eq. 8)}$$

An area the pressure is working on gives the forces that are present to the piston effect. Using Hooke's law the length change due to piston effect, ΔL_1, is given by equation 9:

$$\Delta L_1 = -\frac{LF_R}{EA_s} = \frac{L}{EA_s} P_i\left(A_i - A_{ni}\right) \qquad \text{(eq. 9)}$$

Length change due to helical buckling, ΔL_2, from Lubinski is for a vertical well. In this thesis the setup is horizontal and length change due to helical buckling is derived from the paper "*Tubing buckling – State of the art*"[7], and given by equation 10:

$$\Delta L_2 = -r^2 \frac{F_E L}{4EI} = -\frac{L}{EA_s}\frac{r^2 A_s}{4I} P_i A_{ni} \qquad \text{(eq. 10)}$$

Length change due to ballooning, ΔL_3, is given by equation 11:

$$\Delta L_3 = -\frac{2v}{E}\frac{P_i}{R^2 - 1} L = -\frac{L}{EA_s} P_i A_i \qquad \text{(eq. 11)}$$

Final equation 11 is obtained by substituting $2v$ equal to one and R^2 equal to A_o/A_i.

1.5 Modulus of elasticity

The modulus of elasticity, E, also known as Young's modulus, is a measure of the stiffness of a material. It is defined as the relationship between the uniaxial stress and the uniaxial strain for elastic deformation and can be derived from Hooke's law[8], equation 12:

$$\sigma = E\varepsilon \qquad \text{(eq. 12)}$$

The stress can be derived from the load working on an area of the material and the strain can be derived from the elongation of the material, shown in equations 13 and 14:

$$\sigma = \frac{F}{A} \qquad \text{(eq. 13)}$$

$$\varepsilon = \frac{\Delta L}{L} \qquad \text{(eq. 14)}$$

2 Experimental work

2.1 Preparations

To reproduce Woods' experiment a tube is needed. Form the theory we know that buckling will occur when the pressure inside of a tube is higher than the pressure outside, if the outside pressure is zero, and there is zero axial stress present. As the length of the tube needs to be great compared to the stiffness, a rubber hose was chosen. The rubber hose is a fuel hose with smooth nitrile rubber as the inner material, and smooth neoprene rubber as outer material with synthetic reinforcement in between the layers of rubber. The hose has an inner diameter of 8 mm, outer diameter of 14 mm, a working pressure of 10 bar and a burst pressure of 20 bar.

At first the hose was connected to the tab with a water pressure of 6 bar at the tube inlet and plugged at the tube outlet. Two valves were also connected at the tube inlet, one to be able to bleed off the pressure, and one to open and close the water from the tab. The hose was lying horizontal on a table. The first observations were expected, as the pressure increased, and the piston force working on the plugged end elongated the hose. To stop the elongation the hose was fixed at the end, and buckling occurred. This was also not that unexpected, but this didn't reproduce the theory Woods presented, as the axial forces are not equal to zero, but a start of the thesis and how to think to be able to reproduce Woods work.

When starting to build the setup, the first thing to do was to make something similar to Woods' apparatus, shown in figure 2, and get a sliding leak-proof fit at the end of the hose. To get a leak-proof fit, the expandable rubber hose was not very suitable. A shaft was fitted with an o-ring seal, and a nipple was inserted and fastened in the end of the hose. Then there was a sliding leak-proof fit. When the hose was pressurized the hose was buckled and drawn together and the nipple was disconnected from the shaft.

To measure the force acting on the hose a force transducer, or a load cell, was connected to the setup. To be able to measure the pressure and to get a more controlled pressure increase a pump and a pressure gauge were also connected to the setup. The first load cell force connected to the setup was a load cell that had a range up to 200 kg, and was very rough compared to the small forces present in this experiment. A new load cell, with an interval from 0 to 100 N, was then connected to the setup instead, giving more reliable results, and thereby the setup was complete and ready to start the tests.

2.2 Description of the setup

The setup used in the experimental work in this thesis is shown in figure 3. The setup is lying horizontal on a table. Outside the rubber hose a plexi tube is present to represent the borehole wall or casing. The pressure gauge and the load cell are connected to a PC, so the pressure inside the rubber hose and the measured force at the end can be logged. The hose can either be pressurized by a pump, or by the water pressure from the tab that has a constant pressure of about 6 bar. To bleed off the pressure when needed, an outlet valve is present. There is a nipple fastened in the end of the rubber hose, and a shaft with an o-ring inside the nipple. The shaft is fastened to the table. The nipple is fastened to the load cell that is also fastened to the table. The inlet to the rubber hose is also fastened to the table, making both ends of the rubber hose fixed. From picture 1 you can see how the load cell is connected to the rubber hose.

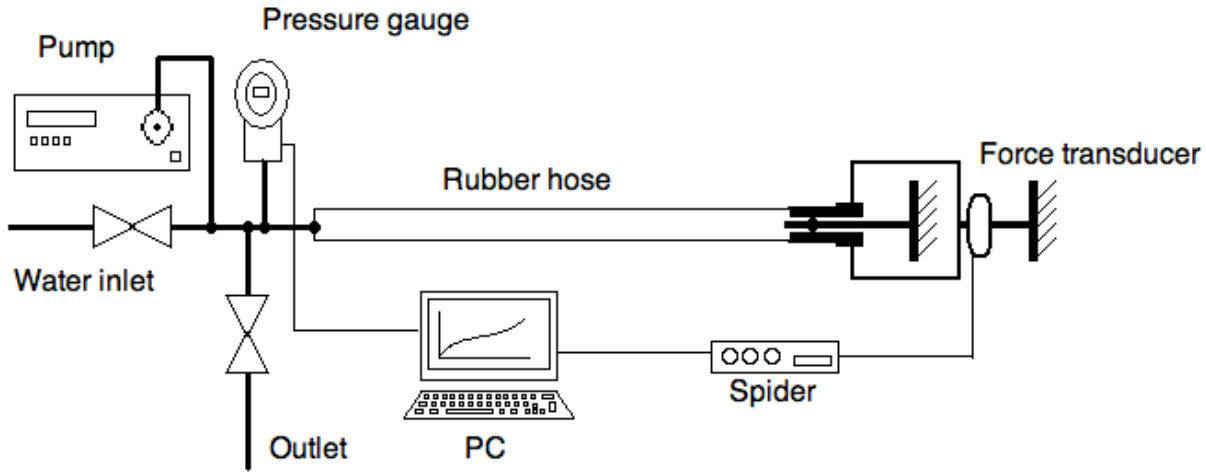

Figure 3: Schematic of the setup.

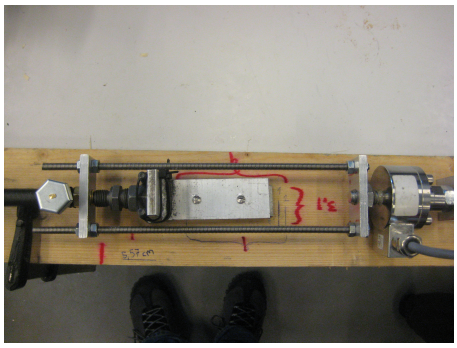

Picture 1: The connection between the load cell and the rubber hose.

In the table below, table 1, there is an overview of the different values for the different parameters in the setup.

Parameter	Value	Unit	Description
A_i	$5{,}03 \cdot 10^{-5}$	m^2	Area of the hose ID
A_o	$1{,}54 \cdot 10^{-4}$	m^2	Area of hose OD
A_{ni}	$3{,}32 \cdot 10^{-5}$	m^2	Area of nipple ID
A_s	$1{,}04 \cdot 10^{-4}$	m^2	X-sect. Area of rubber
R	1,75		Ratio OD/ID hose
r	0,016	m	Hose to plexi tube radial clearance
L	3,97	m	Length of hose
w	0,14	kg/m	Tubing weight pr unit
I	$1{,}68 \cdot 10^{-9}$	m^4	Second moment of inertia
v	0,5		Poisson's ratio

Table 1: Values from the setup.

As we see the Poisson's ratio, v, is assumed to be 0,5. This is because rubber normally has a Poisson's ratio of 0,5 [9]. The Poisson's ratio is needed when the length change due to ballooning is to be calculated.

2.3 Equipment

2.3.1 Pump, Gilson, Model 303

The pump is needed to get a controlled pressure increase inside the hose. The pump rate is set manually. The pump can deliver pressures up to hundreds of bars, but in the experiments conducted in this thesis only a pump pressure up to 10 bar is needed. The pump can't be set to a high-pressure limit at 10 bar, so the pressure from a pressure gauge is needed have control over the pressure. The pump is shown in picture 2.

Picture 2: Pump.

2.3.2 Pressure gauge, Rosemount

The pressure gauge used in this thesis is a pressure gauge from Rosemount and measure the pressure with a certainty of 3 digits. A program called Labview is used to get the pressure logged on a PC. The pressure gauge is shown in picture 3.

Picture 3: Pressure gauge.

2.3.3 Force Transducer, HBM U9B 0,1 kN

The force transducer, or load cell, used for measure the forces is from HBM and has an interval from 0 – 100 N, can measure forces both in compression an in tension. The sensitivity of the force transducer is 1 mV/V. The force transducer is shown in picture 4.

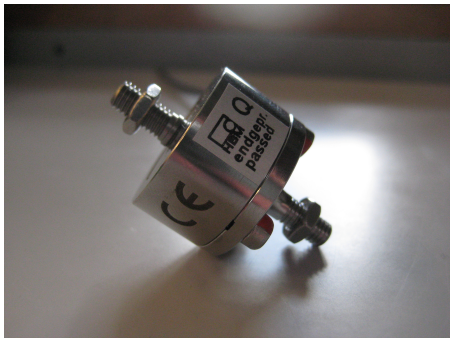

Picture 4: Force transducer.

2.3.4 Spider8

The Spider8 is an amplifier for the signal from the force transducer, and is connected to a PC. A program called Catman 4,5 Professional is used to get a real time graph over the measured force. The spider 8 is shown in picture 5.

Picture 5: Spider8

2.3.5 Rubber hose

The tubing in this thesis is a rubber fuel hose with smooth nitrile rubber as the inner material, and smooth neoprene rubber as outer material with synthetic reinforcement in between the layers of rubber. The hose has an inner diameter of 8 mm, outer diameter of 14 mm, a working pressure of 10 bar and a burst pressure of 20 bar. The length of the hose is 397 cm.

2.3.6 Plexi tube

The plexi tube is representing the casing or borehole wall in a well. The plexi tube is transparent so the rubber hose inside can be seen. The plexi tube however is not sealed to the atmosphere and can't be pressurized, so there is not any external pressure. The ID of the plexi tube is 4,6 cm

2.4 Results from the buckling experiments

The different experiments that are conducted:

- A simple test with water pressure from the tab that has a pressure of approximately 6 bar.
- A test where the pressure is increased to 10 bar to see how the measured force changes
- A test with a small piece of the hose, and a full-length hose to find the o-ring friction force.
- Buckling tests that are repeated to find lateral buckling limit, helical buckling limit and the pitch.
- A test to determine the elasticity modulus of the rubber hose.

2.4.1 Test 1

The first experiment was to see how the setup worked and to observe what would happen when the pressure inside the hose was increased. From figure 3 a schematic of the setup is shown.

The first thing to test is to see if there will be buckling when the hose is pressurized. Water pressure of approximately 6 bar shows that the hose will go straight into helical buckling when the valve to the water is opened. From this we know that the pressure inside the hose, need to be less than 6 bars to get helical buckling.

To get more control over the pressure increase and when the buckling occurs the hose is pressurized with a pump. The rate is kept to 5 ml/min and this rate gives a slow pressure increase. Observation show, as the pressure, P_i, increases, the force measured at the end of the hose, *MF*, increases linear until lateral buckling occurs. The total force works in the direction that puts the hose in tension. The measured force will still increase in almost the same trend, not as steep as before, until the helical buckling occurs. When helical buckling occurs the measured force decreases and the total force changes direction, and work in the direction that puts the hose is in compression.

The results from the test are shown in diagram 1. In diagram 2 are the results from the same test where the measured force is plotted against the pressure instead of time.

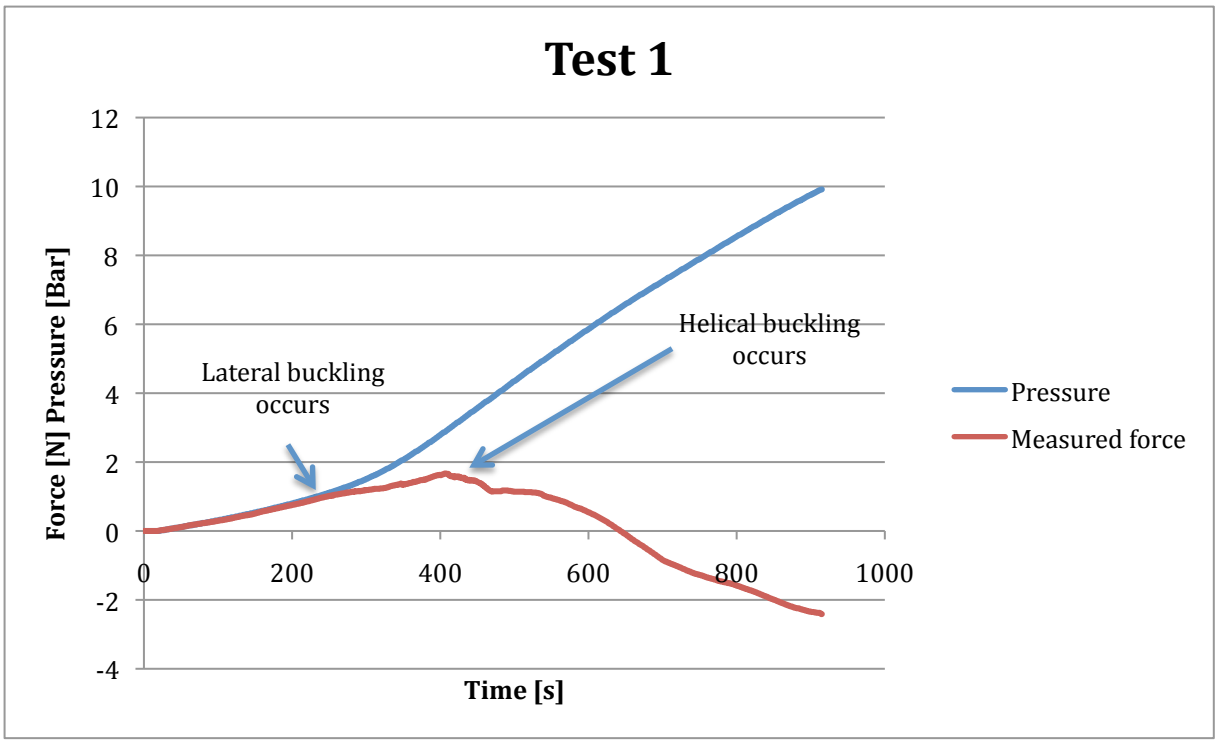

Diagram 1: A test with pressure increase and how the measured force depends on it.

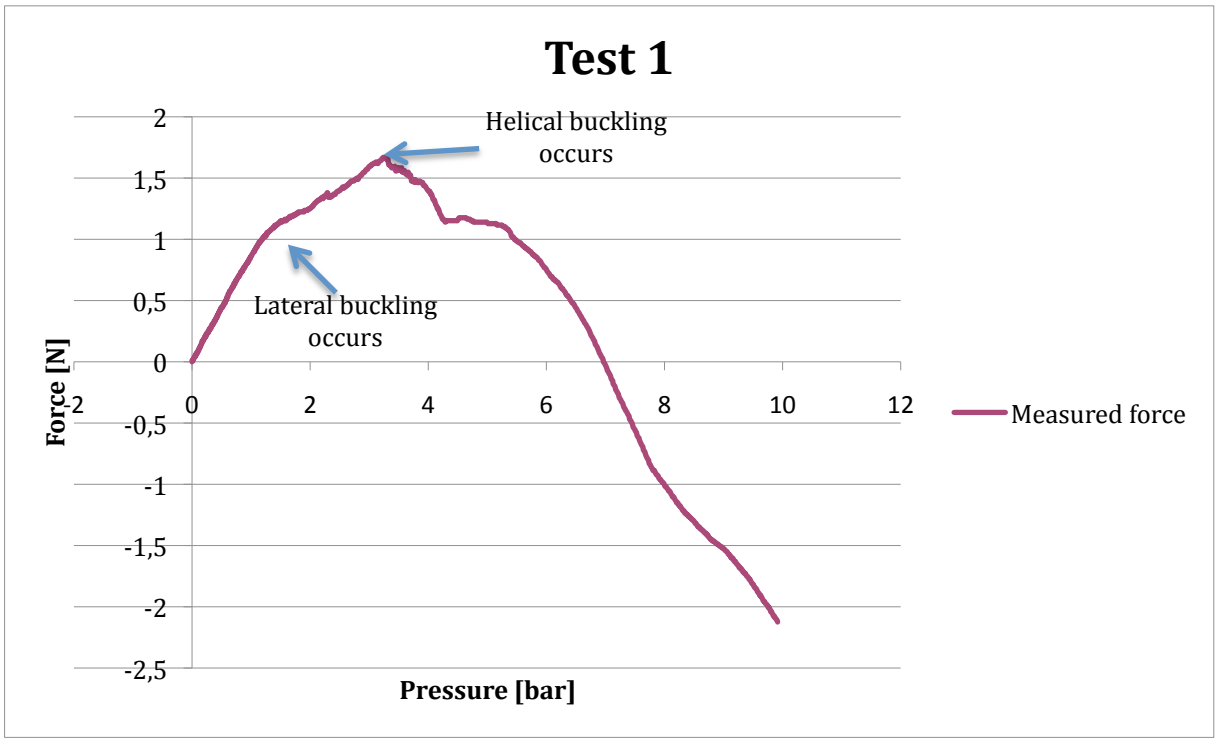

Diagram 2: The same test as in diagram 1 where the measured force is plotted against the pressure.

This test shows the pressure increase until the pressure is 10 bar and how the measured force changes as the pressure increases. Lateral buckling occurs when the pressure is about 1,1 bar, and helical buckling occur when the pressure is about 2,9 bar. The measured force is respectively 1,05 N and 1,65 N, and the real force, piston force, is then -1,88 N and -4,96 N calculated from equation 6.

2.4.2 Determine the o-ring friction force, F_{fric}

In the experimental setup shown in figure 3, both ends of the rubber tube are fixed. A reactive force is generated where the load cell is attached to the tube end. When the pressure is applied. This is discussed later in the thesis, and the reactive force is given by equation 20. The friction force between o-ring and nipple is the difference between applied forces and the measured force as shown in equation 15:

$$F_{fric} = P_i(A_i - A_{ni}) + P_i A_{ni} - MF = P_i A_i - MF \qquad \text{(eq. 15)}$$

To determine the unknown force, F_{fric}, or o-ring friction force, a small piece of the rubber hose, only 10 cm, replaced the full-length rubber hose. The pressure and the measured force were both at zero when the tests started. The pressure was increased with the pump to 10 bar at different rates. The measured force increases as the pressure increases. The measured force is plotted against the pressure in diagram 3. As we plot the pressure against the friction we see from the graph below, diagram 4, that the there is a linear correlation between pressure and friction. For this case the friction is 4,2 N/bar.

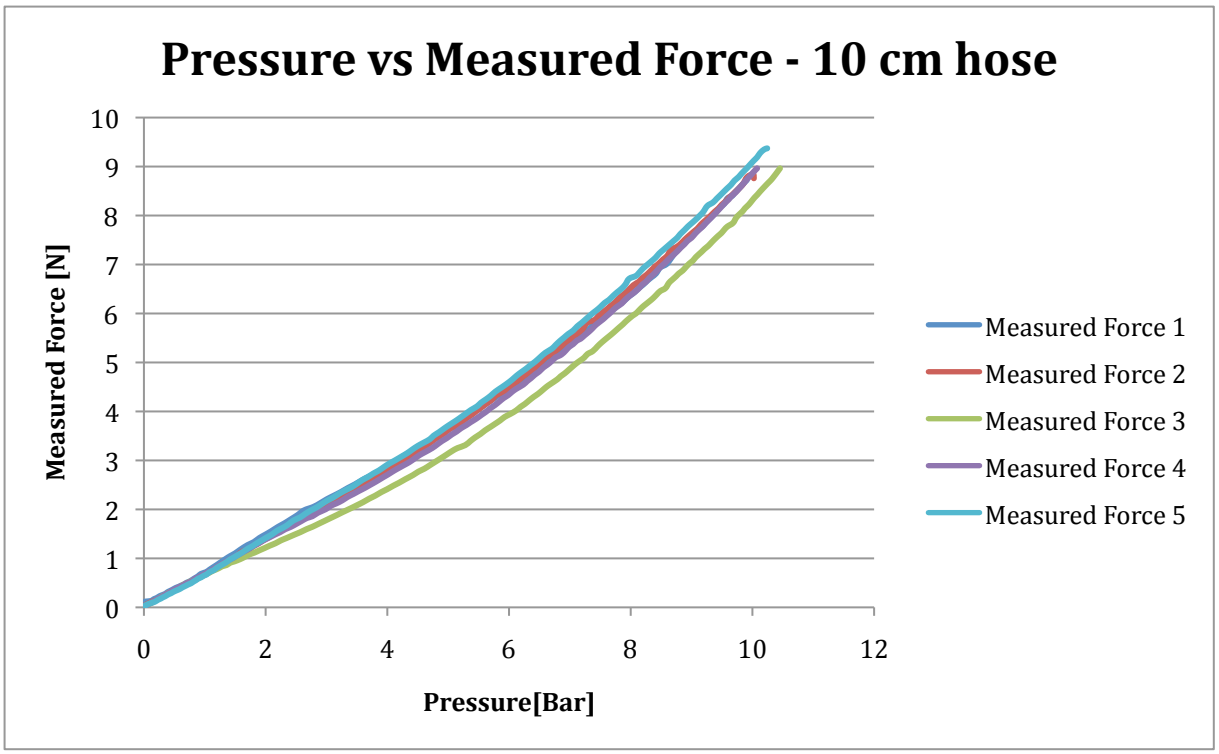

Diagram 3: Measured force plotted against the pressure.

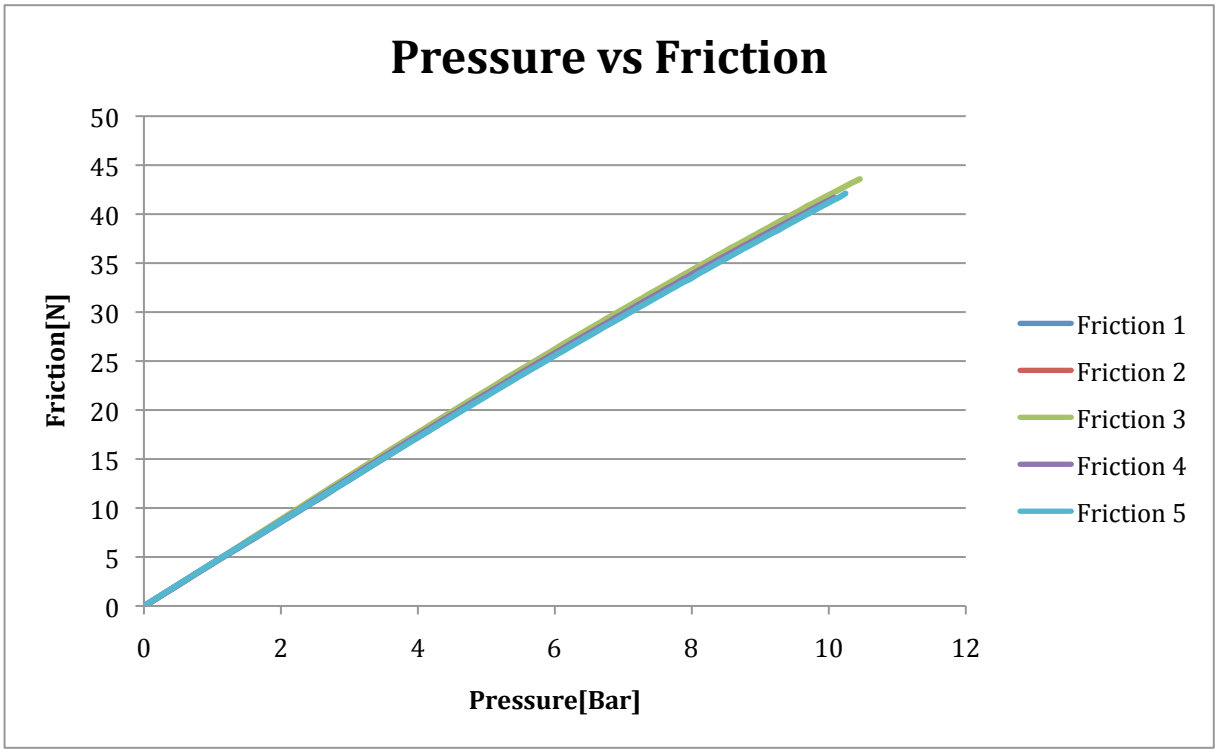

Diagram 3: Pressure versus friction for a small piece of the rubber hose.

This test was also done with the full-length rubber hose. The same procedure was followed only with a bit higher flow rates. The pump was stopped when helical buckling occurred because the values after helical buckling were not representative for the friction force. In the graph below, diagram 5, we can see the measured force plotted against the pressure for the full-length hose.

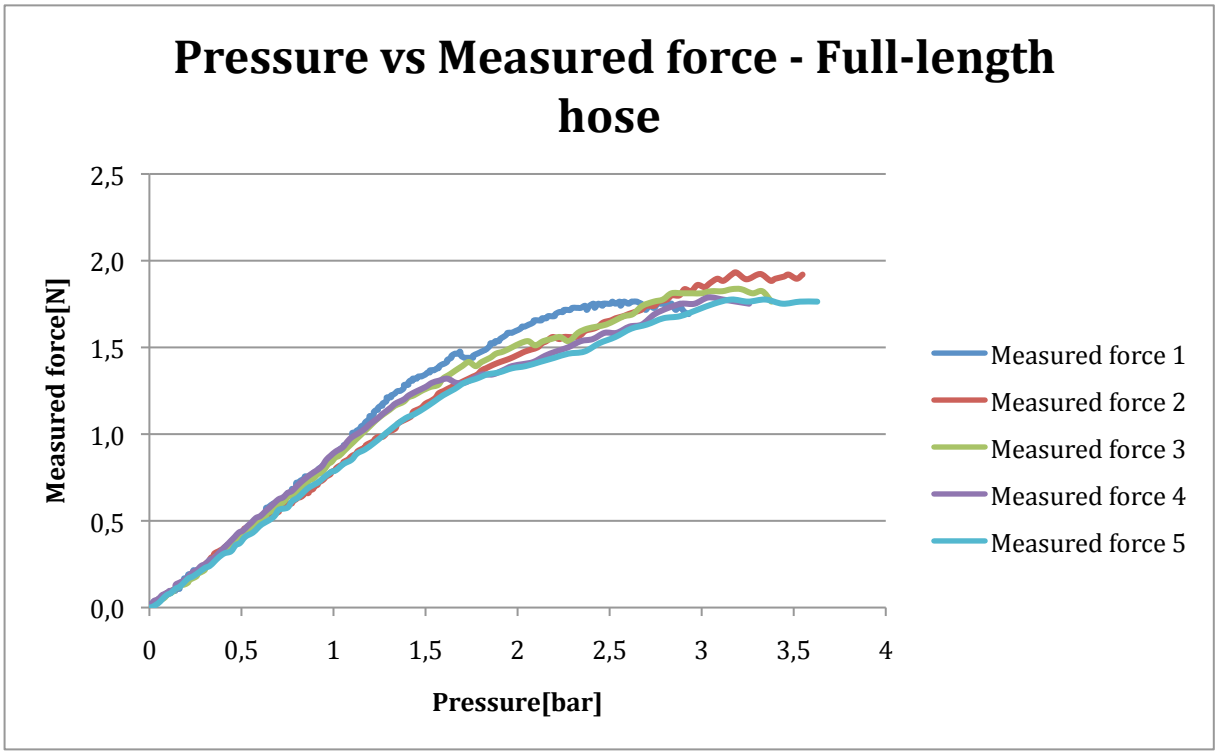

Diagram 5: Pressure versus the measured force for the full-length hose.

In the graph below, diagram 6, we see that there is still a linear correlation between the pressure and the friction. However in this case the friction is a bit higher and is 4,4 N/bar.

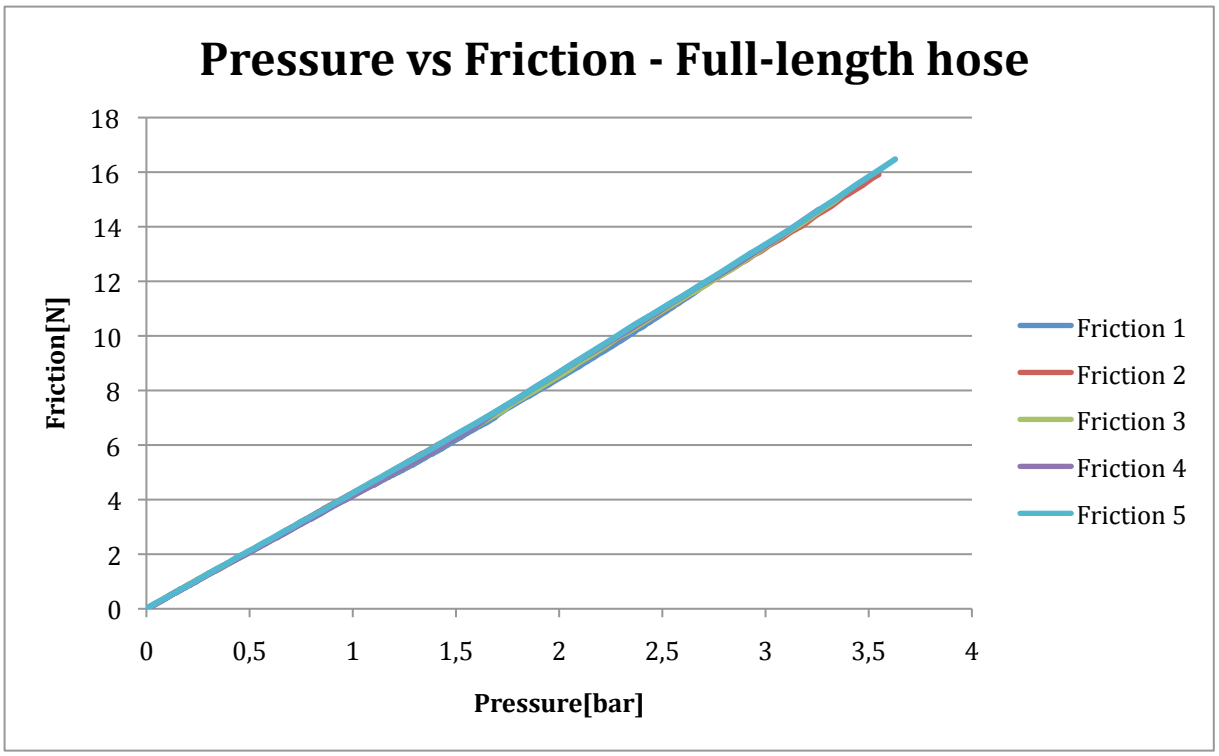

Diagram 6: Pressure versus friction for the full-length rubber hose.

The reason why the friction has a linear correlation and the measured force don't is because of the piston force is large compared to the measured force.

The test was done with a small piece of the hose at first to test the o-ring friction when helical buckling did not occur. With a small piece of the hose nothing of the hose was in contact with the plexi tube, so there was not any friction loss due to the hose was in contact with the plexi tube. The full-length hose was also tested the same way to see if there was a big difference to the o-ring friction in the test with the small piece of the hose. There was a little difference, but not that big. The full-length hose had contact with the plexi tube when the test was conducted.

2.4.3 Buckling tests

More buckling tests that were conducted are tests where the pressure is increased and the measured force is logged. From this we want to detect where the lateral buckling and the helical buckling occur. The pitch is also measured where the lateral buckling occur, the helical buckling occur and when the pressure in the hose is 10 bar. From the graph below, diagram 7, the results from six tests are shown. The pressure was increased with a pump with a flow rate at 5 ml/min. In table 2 you can also see when lateral buckling and helical buckling occurs, and in table 3 you can see the pitch for the different test.

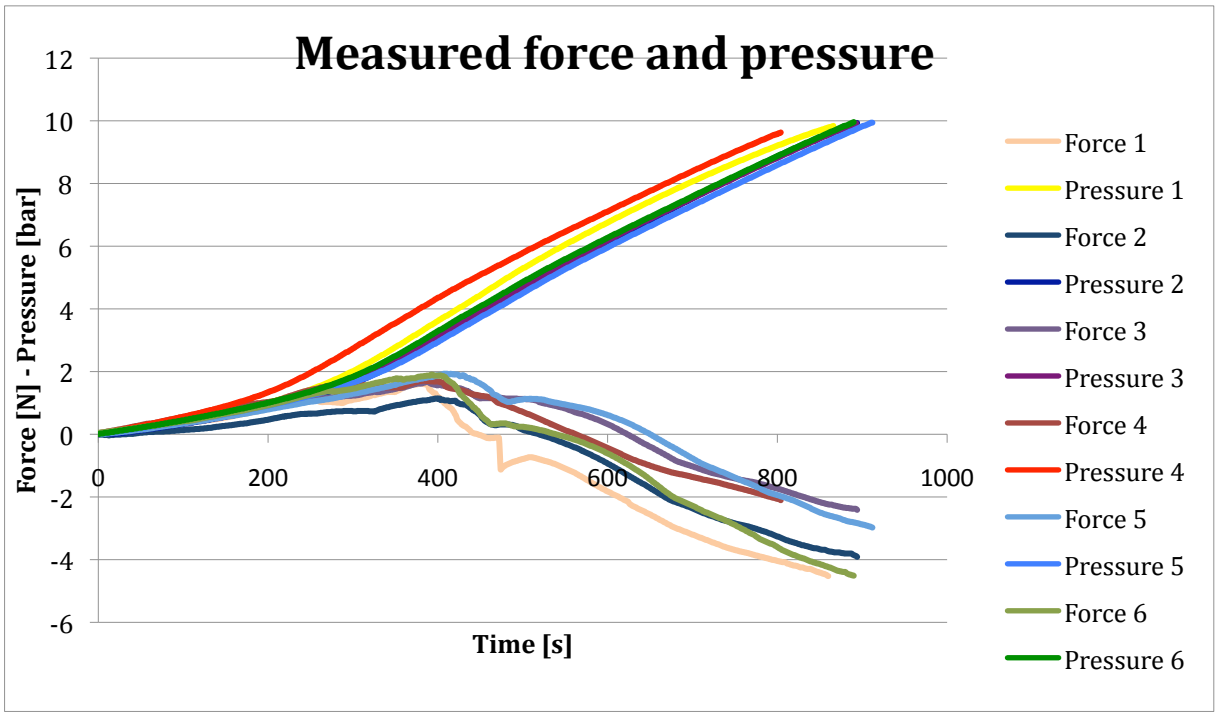

Diagram 7: Buckling tests.

	Lateral buckling starts		Helical buckling starts	
	Force [N]	Pressure [Bar]	Force [N]	Pressure [Bar]
Test 1	1,30	1,76	1,63	3,44
Test 2	0,66	1,12	1,14	2,99
Test 3	1,03	1,13	1,67	2,89
Test 4	0,98	1,02	1,59	2,53
Test 5	1,08	1,31	1,93	3,09
Test 6	1,37	1,56	1,88	3,29

Table 2: Pressure and measured force at lateral and helical buckling.

From the several buckling tests we can see that the average measured force when lateral buckling occurred is 1,07 N and the average pressure is 1,32 Bar. When helical buckling occurred the average measured force is 1,64 N and the average pressure is 3,04 Bar. We see that these values also can be compared with the results for the lateral buckling limit and helical buckling limit from test 1.

	Pitch measured at 10 bar [cm]	Pitch when lateral buckling occur [cm]	Pitch when helical buckling occur [cm]
Test 1	45	51	48
Test 2	43	50	47
Test 3	40	47	44
Test 4	41	48	45
Test 5	38	46	44
Test 6	42	47	45

Table 3: Pitch at 10 bar, when lateral buckling occur, and when helical buckling occur.

From the buckling tests we can see that the average pitch when lateral buckling occurred is 48 cm, the average pitch when helical buckling occurred is 45,5 cm, and the average pitch at 10 bar is 41,5 cm.

From picture 6 below you can see how the rubber hose is in helical buckling inside the plexi tube.

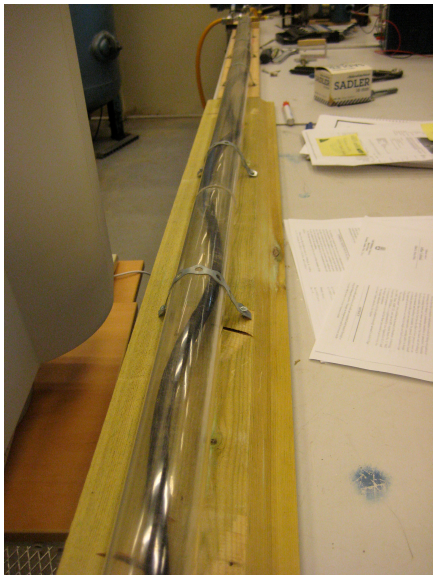

Picture 6: A buckling test where helical buckling occur.

2.4.4 Determine Elasticity modulus

The elasticity modulus is an important factor in many of the equations that are used in the buckling theory. This is tried to determine for the rubber hose to be able to know the magnitude of this factor and to be able to remove an unknown from the equations. To determine Young's modulus for the rubber hose a load was attached to stretch the hose, and the elongation of the hose was measured. This is a measure of the stiffness of the hose in tension, and not in compression. Using Hooke's law from equation 12 and to find the stress and strain from equation 13 and 14, Young's modulus can be determined.

From this test the Young's modulus was determined to be 7 MPa. From different tables an approximation of Young's modulus of rubber was between 10 and 100 MPa[9]. The estimated value from the test is a little lower than this, but in the same magnitude. Table 4 shows the results from the test. The area of the rubber hose wall was assumed to be constant.

Load [Kg]	Force [N]	Area [mm^2]	Stress [kPa]	ΔL [cm]	Strain [10^{-6}]	E-modulus [MPa]
0,5	4,91	103,7	47,3	2,9	7286	6,5
1	9,81	103,7	94,6	4,8	12060	7,8
2	19,62	103,7	189,2	11,1	27889	6,8
3	29,43	103,7	283,9	14,9	37437	7,6
3,5	34,34	103,7	331,2	20,2	50754	6,5
6,78	66,51	103,7	641,6	36,0	90452	7,1

Table 4: Results from the testing of the elasticity modulus.

3 Discussion

3.1 Woods' experiment

The axial stress is zero in Woods' experiment. Since the force is measured at the end of the hose, and this measured force is not equal to zero we see that the axial stress is not zero due to exposed nipple area. A screw mechanism to remove the axial stress mechanical was installed in the setup. This was put on the shaft in the end of the hose, and was suppose to be screwed against the hose when the stress occurred. The measured force before helical buckling was acting in the direction so the hose was in tension, and with the screw mechanism the measured force was suppose to be equalized. When the forces were equalized there would be zero axial stress, and then we could see if buckling occurred at once the hose was pressurized. The problem with this mechanism was that the measured force was so little, and with just a little adjustment on the screw mechanism the measured forces was not equalized, but it was working in the other direction with a much higher force. So there was not any useable data collected from these tests.

One of the main differences between Woods' experiment and the experiment conducted in this work is boundary conditions at the tube end. Woods considered a free-moving response while in the present work the tube end is attached to a load cell. The case that Woods considered is similar to a production tubing terminated in a sliding packer to tubing arrangement. The case considered in the present work is closely related to a fixed packer where the tubing end has no room for movement.

3.2 Comparison of the theory and the experimental tests

3.2.1 Modifications using Lubinski packer force theory

The response at the force transducer depends upon ΔL_1, ΔL_2 and ΔL_3 discussed before. If there is no buckling, the length change due to helical buckling doesn't apply, and the total length change is given by equation 16:

$$\Delta L_6 = \Delta L_1 + \Delta L_3 = -P_i \frac{L}{EA_s} A_{ni} \qquad \text{(eq. 16)}$$

The corresponding ΔL_p needed to keep the tube end in place is given by equation 17:

$$\Delta L_p = -\Delta L_6 = P_i \frac{L}{EA_s} A_{ni} \qquad \text{(eq. 17)}$$

The fictitious length change, ΔL_f is given by equation 18:

$$\Delta L_f = -P_i \frac{L}{EA_s} A_{ni} \qquad \text{(eq. 18)}$$

And the overall Length change, ΔL_{pf}, is given by equation 19:

$$\Delta L_{pf} = \Delta L_p + \Delta L_f \qquad \text{(eq. 19)}$$

We see from equation 18 and 19 that ΔL_p and ΔL_f cancel each other and the overall length change is zero. Since the overall length change is zero, the fictitious force caused by the end constraint is zero as well. The "tube to load cell force", or packer force, is given by equation 20:

$$F_p = -F_f = -P_i A_{ni} \qquad \text{(eq. 20)}$$

The corresponding axial force in the tube is given by equation 21:

$$F_{ap} = F_a + F_p = -P_i A_i \qquad \text{(eq. 21)}$$

These equations above are applicable prior to buckling. For the case of developed helical buckling, ΔL_2 is applied to the total length change and the corresponding length needed to keep the tube end in place is given by equation 22:

$$\Delta L_p = -\Delta L_6 = P_i \frac{L}{EA_s} \frac{4I + r^2 A_s}{4I} A_{ni} \qquad \text{(eq. 22)}$$

The fictitious length change is given by equation 23:

$$\Delta L_f = -P_i \frac{L}{EA_s} \frac{4I + r^2 A_s}{4I} A_{ni} \qquad \text{(eq. 23)}$$

Again we see that ΔL_p and ΔL_f cancel each other. The conclusion is that the expected end response with and without helical buckling is identical. In this study there is clearly a change before and after buckling.

3.2.2 Buckling limits

The tests shows that the average measured force when lateral buckling occurs is 1,07 N, and the average measured force when helical buckling occurs is 1,64 N. When the lateral and helical buckling occur is found when observing the hose, and there might be some uncertainties in these values. There might be a discussion on exactly when the lateral or helical buckling occurs, and this might also be a personal preference to when this happens. In this thesis however it is seen that when lateral and helical buckling are observed, there is also a change in the slope of the measured force, and this might be a good indication that the observed limits are not far from the truth. Also there are conducted a lot of tests and an average value has been used for the calculations.

From equation 6 and 7 we can find the real and effective force from the measured force. The real force when lateral and helical buckling occurs is respectively -2,26 N and -5,20

N. The effective force is 4,38 N when lateral buckling occurs and 10,09 N when helical buckling occurs.

When calculating *LBL*, HBL_1, and HBL_2, from equations 1, 2 and 3, the values are a little off from the ones found in the experiments. *LBL* is calculated to be 2,01 N, HBL_1 is calculated to be 2,84 N and HBL_2 is calculated to be 5,68 N. This is when we assume that the value found for the Young's modulus in chapter 2.4.4 is correct, thus 7 MPa. The effective force when lateral buckling occurs is twice as much as the lateral buckling limit, It is expected to be a little higher, but not the double. The effective force when helical buckling occurs is almost twice the value of the second helical buckling limit. It is expected to be in between these two helical buckling limits.

If we consider the relation between HBL_1 and *LBL* the value is 1,41 and if we consider the relation between HBL_2 and *LBL* the value is 2,83. The relation between the observed helical buckling limit and the observed lateral buckling limit is expected to be within this interval. The relation between the observed helical limit and the observed lateral limit is 2,30 and within this interval.

3.2.3 Length changes

The length changes, ΔL_1, ΔL_2 and ΔL_3, is calculated from equation 9, 10 and 11. Before helical buckling or when lateral buckling occurs, $P_i = 1{,}32$ *bar*, only ΔL_1 and ΔL_3 are present. At this pressure ΔL_1 is calculated to be 1,2 cm and ΔL_3 is calculated to be -3,6 cm where negative length change is contraction of the hose. The total length change, ΔL_6, is then -2,4 cm. This is calculated when Young's modulus is 7 MPa. This is a bit strange since the force transducer at the end shows a force that the hose is in tension. The hose is fixed at the end, like an integral packer in a well. The hose doesn't move, but these are the calculated length changes that we would see on the hose if the hose had a free motion end.

From the preparations, chapter 2.1, we remember that the hose was elongated when the hose was pressurized. The whole inner area, A_i, of the hose was then plugged, and if we consider the total length change for this case it is calculated to be zero. There is no

buckling in this case and ΔL_2 is not applied for the total length change. But the total length change is not zero, it is measured to be 11 cm. The assumption that Poisson's ratio is equal to 0,5 might be a bad assumption.

At the pressure when helical buckling occurs, $P_i = 3{,}04$, ΔL_2 is also applied to the total length change. The total length change at this pressure is – 27,3 cm. At this point the load cell shows the largest force in the direction that the hose is in tension. After ΔL_2 is applied the measured force changes direction and the hose will contract. From test 1, diagram 2, we see that the measured force is equal to zero at about 7 bar. At this pressure the total length change is calculated to be -62,9 cm. This is very strange. The hose is not believed to have a theoretical length change of 63 cm in contraction and since the measured force is equal to zero the total length change would be expected to be the same as when the test started, i.e. zero.

3.2.4 Pitch

The pitch at helical buckling is calculated to be 30 cm, when Young's modulus is set to be 7 MPa. From the test we see the pitch has an average at 45,5 cm. The pitch from the tests is measured with a ruler. There might be some uncertainties in these measurements as well since the pitch is not constant all over the hose. The pitch is not larger in one end and smaller in the other end, but differ a little bit over the whole hose. The pitch measured from each test is taken out of an average pitch, and since many different tests are conducted, and an average pitch of these tests is used, the measured pitch is considered to be close to the truth. Since the calculated pitch doesn't correlate with the measured pitch it might be because of a wrong value for Young's modulus.

From the test the pitch is measured when lateral buckling occurs, helical buckling occurs, and when the inside pressure is 10 bar. Not unexpected the pitch is getting smaller as the pressure increases. When the pressure approaching 10 bar, there is almost no change in the pitch.

3.3 Young's modulus

As we take a look at the first test, test 1, where the pressure is increased, and the force is measured the pressure does not get a linear increase before there is about 2 bar inside the hose. This is probably because the hose is expanding, and the volume inside the hose is increasing and the pressure inside the hose doesn't increase that much in the beginning. Due to this expanding of the hose there might be a change in Young's modulus because the hose get stiffer at higher inside pressures.
Equations where the Young's modulus is a parameter shows that there is natural to question the value for Young's modulus from the test. Equations as the helical buckling limits, the pitch and the length change due to helical buckling, respectively equation 2, 3, 4 and 10, has Young's modulus as a parameter.

From these equations using the Young's modulus found at 7 MPa the pitch would be 30 cm, the HBL_1 would be 2,84 N, the HBL_2 would be 5,68 N and the length change due to helical buckling would be -21,8 cm. These values are calculated when helical buckling occurs, when $P_i = 3{,}04$. From the test that is conducted we can see that the average pitch is 45,5 cm and the helical buckling limit is 10,09 N. The length change due to helical buckling is not that easy to see because the hose is fixed in both ends, but 22 cm in contraction seems a bit high. If Young's modulus were higher, 2 times higher, the pitch and length change due to helical buckling would correspond more to the results from the experiment. The helical buckling limit found from the experiment would also be closer to the calculated helical buckling limits. The table below, table 5, show how the calculated values match the results found from the experiment at different values for Young's modulus. When Young's modulus is 3 times as big as the one found in the test the calculated values seems a bit large.

E [MPa]	$\Delta L2$ [cm]	p [cm]	LBL [N]	HBL_1 [N]	HBL_2 [N]
7	21,8	30	2,01	2,84	5,68
14	10,9	43	2,84	4,02	8,04
21	7,6	53	3,48	4,92	9,84
Results from the experiment:		46	4,38	10,09	10,09

Table 5: Calculated values for different E-values.

In the preparation there is explained that when pressurized with water at 6 bar the hose elongated. This elongation was 11 cm and if we want to compare this to find the Young's modulus. Using the theory for modulus of elasticity, Young's modulus is in this case calculated to be 10,5 MPa.

When determining Young's modulus the area was assumed to be constant, and this is not entirely true when the hose is elongated. Young's modulus was also determined for the hose in tension, and this may differ from the value for Young's modulus in contraction.

4 Conclusion

To reproduce Woods' experiment a lot of time was used to build a setup to minimize the axial stress. The setup was improved all the time to be able to get the best results possible. Since real life differ from the theory it was difficult to remove the friction from the setup, and to create a sliding leak proof fit that could remove all the axial stress.

The theory for the calculated length change doesn't seems to be a very well match for this thesis. The buckling limits found from the experiment are also a bit high to what was expected. It seems that the theory from Lubinski, which is proven for steel pipes, doesn't apply for a rubber hose. It is often assumed that rubber has the same elastic behaviour as metal, but this is a bad assumption. Rubber has strain energy stored thermally, while metal has strain energy stored electrostatic[10]. In steel pipes the strain in compression is the same as the strain in tension. It is recommended that a similar study used with a metal tube instead need to be conducted.

The Young's modulus is believed to be a little low compared to what is determined. When assuming Young's modulus to be 2 times higher the values from the experiment matched better with the results from the experiment.

It would be really interesting to take this experiment further and scale it up and try to use a metal pipe of any kind instead of a rubber hose.

5 References

[1] J. M. Ra. 2005. Experimental study of buckling analysis in vertical and near vertical wells. Master thesis at UiS.

[2] R. Dawsonand P.R. Pasley 1984. Drillpipe buckling in inclined holes.

[3] Y. Chen et. al. 1990. Tubing and casing buckling in horizontal wells.

[4] S. Miska and J.C. Cunha. 1995. An analysis of helical buckling of tubulars subjected to axial and torsional loading in inclined wellbores.

[5] A. Klinkenberg. 1951. The neutral zones in drill pipe and casing and their significance in relation to buckling and collapse.

[6] Stefan Miska. 1962. Developments in petroleum engineering.

[7] R. F. Mitchell. 2006. Tubing buckling – State of the art. SPE- paper 104267.

[8] W. D. Callister jr. 2007. Materials science and engineering, an introduction.

[9] http://www.engineeringtoolbox.com. Link found 02.06.2010

[10] http://en.wikipedia.org/wiki/Natural_rubber. Link found 10.06.2010